Damping Functions and Chain Relaxation in Uniaxial and Biaxial Extensions: Comparison with the Doi–Edwards Theory

O. Urakawa

Department of Polymer Science and Engineering, Kyoto Institute of Technology, Matsugasaki, Sakyo-Ku Kyoto 606, Japan

M. Takahashi,* T. Masuda, and N. Golshan Ebrahimi

Department of Material Chemistry, Faculty of Engineering, Kyoto University, Yoshida, Sakyo-Ku Kyoto 606, Japan

Received March 8, 1995; Revised Manuscript Received July 25, 1995®

ABSTRACT: Damping functions for polystyrene melts with narrow and broad molecular weight distributions were obtained from step-strain stress relaxation experiments in shear and biaxial extension. A lubricated squeezing flow method was used to obtain the biaxial relaxation modulus. Following the Wagner method, we calculated the damping function in uniaxial extension from experimental data on the stress growth coefficient. The calculated damping function was independent of strain rate. In all deformation modes, strain dependences of the damping functions for narrow distribution polystyrene were stronger than those for broad distribution polystyrene. Experimental damping functions for narrow distribution polystyrene were compared with predictions of the Doi–Edwards theory. The predicted shear damping function agreed well with the experimental data. Fair agreement between the predictions and the data was observed in uniaxial and biaxial extensions. Compared at the same Hencky strain, the component of the radius of gyration tensor in the stretching direction is greater for uniaxial extension than for biaxial extension. However, stretching of the primitive chain along the contour is more prominent in biaxial extension than in uniaxial extension, giving a stronger damping (contraction of the primitive chain) in biaxial extension. This explains the stronger strain dependence of the biaxial damping function.

I. Introduction

Many studies have been reported on stress relaxation behavior in shear after application of a finite step strain in entangled polymer systems. Experimental results for the shear relaxation modulus were reviewed by Osaki.[1] The shear relaxation modulus $G(t,\gamma)$ decreases with increasing shear strain γ, and at long times the following time–strain separability is observed:[1,2]

$$G(t,\gamma) = G(t)\, h(\gamma) \tag{1}$$

where $G(t)$ is the linear relaxation modulus and $h(\gamma)$ is a damping function. Osaki classified the behavior of $h(\gamma)$ into three types A, B, and C.[1] Entangled flexible polymers with narrow molecular weight distributions (MWDs) show type A behavior, in which $h(\gamma)$ is almost a universal function of γ and is independent of molecular weight and concentration. The Doi–Edwards (DE) theory[3–5] describes this functional form of $h(\gamma)$ very well.

Other polymers show a weaker strain dependence (type B) than narrow distribution polymers: Polymer systems with broad MWDs, polymers having multiple branch points, and nonentangled polymers belong to this class, and the types of behavior are classified as B1, B2, and B3, respectively. One explanation for the weaker damping of multiple branch polymers was proposed by Larson.[6] He surmised that the chain section connecting the branch points does not easily relax (the snap back to the equilibrium length is suppressed). No theoretical explanation has been given for the effect of a broad MWD on the behavior of damping function $h(\gamma)$. For highly entangled systems with more than 50 entanglement points per molecule, the strain dependence of $h(\gamma)$ becomes very much stronger than that of type A. This behavior is classified as type C. Marrucci, argued theoretically that this behavior arose from an instability effect under large strains.[7]

Applicability of the DE theory is limited to narrow MWD samples with also an appropriate range of molecular weights. At short times, eq 1 does not hold due to the existence of a fast relaxation process, which is not observed under the small strain condition. The contribution of this fast process becomes greater with increasing strain γ. This behavior is also well explained by the DE theory.[8] The fast relaxation process has been considered to be contraction (retraction or snap back) of the stretched primitive chain.[3–5]

The DE theory has been validated in the case of shear deformation. Difficulty in experiments has prevented evaluation of the model in other deformation modes. Thus it is important to carry out exact measurements in extensional deformations in order to test the possibly wide applicability of the model. Soskey and Winter,[9] and then Khan, Prud'homme, and Larson,[10] investigated the equi-biaxial stress relaxation behavior of polymer melts with a lubricated squeezing flow method. However, the samples they used belong to the category of type B. Further, in the latter investigation data for the biaxial relaxation modulus were limited to the short time region only. The time range was 10 times narrower compared with the shear relaxation modulus. Wagner[11,12] proposed a clever way to obtain damping functions in extensional flows which can be calculated by applying a general form of the BKZ type constitutive equation.[13] Using published data by Demarmels and Meissner[14] on extensional flows for a polyisobutylene melt with a broad MWD, he obtained damping functions and compared them with the DE theory. Both data sets (Khan–Prud'homme–Larson and Demarmels–Meissner) showed weaker dampings than the theoretical predictions. However, as already mentioned, the broadness of the MWD leads to a weaker strain dependence

® Abstract published in *Advance ACS Abstracts,* September 15, 1995.

0024-9297/95/2228-7196$09.00/0

for the damping functions. At present, the real strain dependence of damping functions for narrow-distribution polymers in extensional flows is not known.

Considering the above situation, we made careful measurements of the biaxial stress relaxation of polystyrene melts with narrow and broad MWDs and obtained the biaxial damping function. We determined the uniaxial damping function from uniaxial extensional viscosity data previously reported[8] through Wagner's method.[11,12] In this paper, we show these damping functions together with the shear damping function which was also obtained in the previous study. These experimental damping functions are compared with predictions of the DE theory.

II. Predictions from the Doi–Edwards Theory

II.1. Contour Length Stretching and Radius of Gyration Tensor. According to the DE theory, each chain in an entangled system deforms affinely upon imposition of a step strain. Such deformed conformations of a primitive chain are characterized by two factors, *i.e.* orientation of bond (tube segment) vectors and stretching of each bond length, resulting in the contour length stretching. After this instantaneous deformation of the primitive chain, the stretched contour length contracts (retracts) to the equilibrium length, giving the fast stress relaxation process or damping in the relaxation modulus. At the final stage, the orientational anisotropy of the bond vectors disappears by reptational motion. The reptation is the same mechanism occurring under the small strain (linear response). For this reason, the separability of $G(t,\gamma)$ in eq 1 holds at long times where reptation is the dominant relaxation mechanism. After all, the stress damping is due to the contraction of the primitive chain, and the contraction determines the damping function $h(\gamma)$.

The stretch ratio of the contour length, α, is expressed by the following equation assuming an affine deformation,

$$\alpha = \langle|\mathbf{E}\cdot\mathbf{u}|\rangle = \langle u'\rangle \tag{2}$$

where $\mathbf{E}$ is the deformation gradient tensor, $\mathbf{u}$ is a unit vector in the direction of a bond vector, and u' is the deformed bond length. The average in eq 2 can be carried out by spatial integration for uniaxial and biaxial extensions, and one obtains analytical solutions. In shear, we calculated α numerically. Analytical expressions for α are

$$\alpha = \frac{1}{2}\lambda\{1 + A(\lambda)\} \qquad \text{for uniaxial extension} \tag{3a}$$

$$\alpha = \frac{1}{2\lambda_B^2}\{1 + B(\lambda_B)\} \qquad \text{for biaxial extension} \tag{3b}$$

where λ and λ_B are the external stretch ratios for uniaxial and biaxial extensions and $A(\lambda)$ and $B(\lambda_B)$ are defined as

$$A(\lambda) = \frac{\sinh^{-1}\sqrt{\lambda^3 - 1}}{\sqrt{\lambda^3(\lambda^3 - 1)}} \tag{4a}$$

$$B(\lambda_B) = \frac{\lambda_B^6}{\sqrt{\lambda_B^6 - 1}} \sin^{-1}\sqrt{\frac{\lambda_B^6 - 1}{\lambda_B^6}} \tag{4b}$$

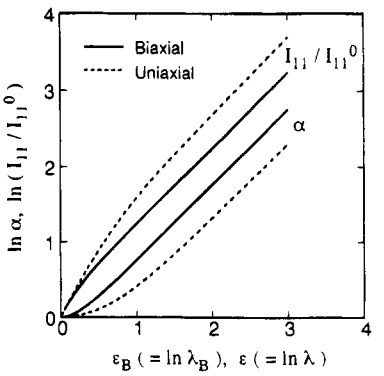

Figure 1. Stretch ratio α of the contour length of a primitive chain and the component I_{11} of the radius of gyration tensor with the stretching direction 1 as functions of the Hencky strains ϵ_B and ϵ in biaxial and uniaxial extensions.

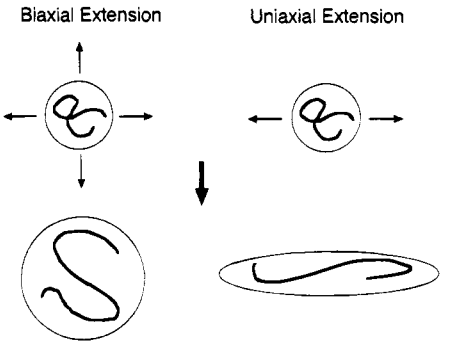

Figure 2. Chain deformation just before and after application of a step strain in biaxial and uniaxial extensions.

The radius of gyration tensor $\mathbf{I}$ is defined by Doi and Edwards,[3] and the change of $\mathbf{I}$ in shear and extensional flows has been calculated by Sekiya and Doi.[15] The tensor $\mathbf{I}$ can be expressed in the following form

$$\mathbf{I} = \langle S_0^2\rangle\mathbf{C}^{-1}/(3\alpha) \tag{5}$$

where $\mathbf{C}^{-1}$ is the Finger strain tensor given by $\mathbf{E}\cdot\mathbf{E}^T$ (T is the transpose) and $\langle S_0^2\rangle$ is the mean square radius of gyration at equilibrium. In Figure 1, the molecular stretch ratio α and a component I_{11} of the radius of gyration tensor with a stretching direction 1 are shown as functions of external stretch ratio (λ and λ_B). The contour length stretching is expressed in terms of a molecular extensional strain $\ln\alpha$ and the macroscopic deformation by the Hencky strain ϵ ($=\ln\lambda$) for uniaxial extension and ϵ_B ($=\ln\lambda_B$) for biaxial extension. In the figure, I_{11}^0 is the equilibrium value of I_{11}, and $I_{11} = I_{22}$ for biaxial extension, where 2 is another stretching direction in biaxial extension. We can see that α in biaxial extension is larger than that in uniaxial extension compared at the same Hencky strain. This causes stronger damping of the relaxation modulus in biaxial extension, because the damping function h is approximately given by $h \approx \alpha^{-2}$ according to the DE theory. In contrast with α, the component I_{11} is smaller in biaxial extension than in uniaxial extension. Considering the differences of α and I_{11} in uniaxial and biaxial extensions, single chain deformation is schematically represented as in Figure 2. This figure illustrates that in biaxial extension, the contour length stretching is stronger but the radius of gyration is smaller in the stretching direction 1. The bond orientation in the stretching direction 1 becomes much weaker in biaxial extension.

II.2. Relaxation Moduli and Damping Functions. The DE predictions for relaxation moduli are

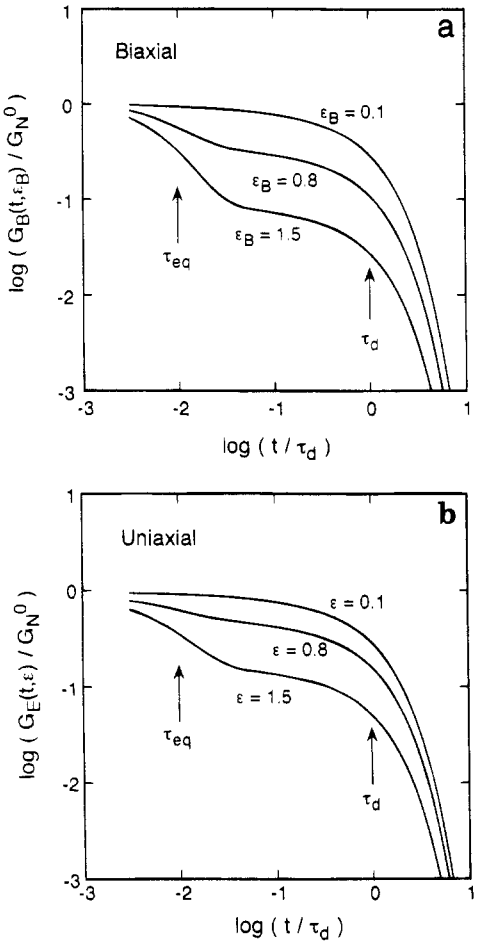

Figure 3. Doi–Edwards prediction on the relaxation modulus for (a) biaxial extension and (b) uniaxial extension. The ratio of relaxation times, τ_d/τ_{eq}, is set to be 100.

shown in Figure 3a,b for biaxial extension $G_B(t,\epsilon_B)$ and uniaxial extension $G_E(t,\epsilon)$. For the contraction process, we did not use the independent alignment (IA) approximation and calculated rigorously. The figures show a case where the disengagement time (maximum relaxation time) τ_d and the equilibrium time (contraction time) τ_{eq} are fairly apart, i.e., $\tau_d/\tau_{eq} = 100$. The relaxation moduli are reduced using the plateau modulus G_N^0. At long times ($t \gg \tau_{eq}$), time–strain separability holds for both moduli.

$$G_B(t,\epsilon_B) = G(t)\, h_B(\epsilon_B) \tag{6a}$$

$$G_E(t,\epsilon) = G(t)\, h_E(\epsilon) \tag{6b}$$

where $h_B(\epsilon_B)$ and $h_E(\epsilon)$ are damping functions. We can see clearly that damping (decrease in relaxation modulus with strain) is stronger in biaxial extension than in uniaxial extension.

We can calculate damping functions in two ways, with and without using the IA approximation. Hereafter, the two ways or the results are denoted as DE(IA) and DE(rigorous). In Figure 4, two assumed ways of contraction (rigorous and IA) are presented for biaxial and uniaxial extensions. The stretched primitive chain contracts along its contour in rigorous contraction. In IA, the chain contracts similarly, preserving the initial orientation as if there were no constraints due to entanglements. We can see clearly from this figure that the difference between the rigorous and IA calculations will be greater for biaxial extension than for uniaxial extension.

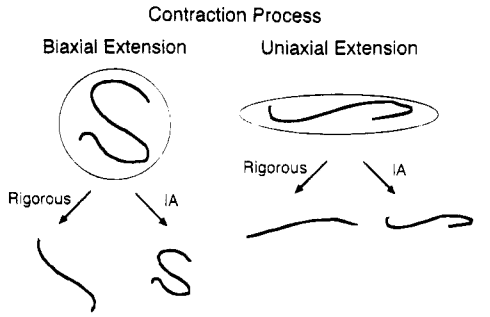

Figure 4. Doi–Edwards assumptions on the contraction process (rigorous and independent alignment) in biaxial and uniaxial extensions.

In rigorous and IA calculations, damping functions are given by the following equations.

$$h = \frac{15}{4\langle u'\rangle}\left\langle\frac{u'_1{}^2 - u'_3{}^2}{u'}\right\rangle\frac{1}{C^{-1}_{11} - C^{-1}_{33}} \qquad \text{(rigorous)} \tag{7a}$$

$$h = 5\left\langle\frac{u'_1{}^2 - u'_3{}^2}{u'^2}\right\rangle\frac{1}{C^{-1}_{11} - C^{-1}_{33}} \qquad \text{(IA)} \tag{7b}$$

Here the subscripts 1–3 are for the vector or tensor components, and the directions of uniaxial and biaxial extensions are 1 and 1, 2, respectively. The integral in eq 7 can be solved analytically. The result for uniaxial extension is

$$h_E = \frac{15}{2}\frac{\lambda^4}{(\lambda^3-1)^2}\left(1 - \frac{\tan^{-1}\sqrt{\lambda^3-1}}{\sqrt{\lambda^3-1}}\right) - \frac{5}{2}\frac{\lambda}{\lambda^3-1} \qquad \text{(IA)} \tag{8a}$$

$$h_E = \frac{15}{8}\frac{\lambda(2\lambda^3+1)}{(\lambda^3-1)^2}\frac{1}{1+A(\lambda)}\left(1 - \frac{4\lambda^3-1}{2\lambda^3+1}A(\lambda)\right) \qquad \text{(rigorous)} \tag{8b}$$

For biaxial extension the damping function becomes

$$h_B = \frac{15}{2}\frac{\lambda_B{}^4}{(\lambda_B{}^6-1)^2}\left(1 - \frac{\lambda_B{}^3\tanh^{-1}\sqrt{(\lambda_B{}^6-1)/\lambda_B{}^6}}{\sqrt{\lambda_B{}^6-1}}\right) + \frac{5}{2}\frac{\lambda_B{}^4}{\lambda_B{}^6-1} \qquad \text{(IA)} \tag{9a}$$

$$h_B = \frac{15}{8}\frac{\lambda_B{}^4(\lambda_B{}^6+2)}{(\lambda_B{}^6-1)^2}\left(1 - \frac{6}{1+B(\lambda_B)}\frac{B(\lambda_B)}{(\lambda_B{}^6+2)}\right) \qquad \text{(rigorous)} \tag{9b}$$

The calculated damping functions in uniaxial and biaxial extensions and in shear are compared in Figure 5. The strong strain dependence of damping functions in extensional flows is due to large stretching and contraction of the primitive chain in these flows. The difference between rigorous and IA calculations is largest in biaxial extension, as pointed out previously.

III. Experimental Section

III.1. Materials. Two polystyrenes with narrow and broad molecular weight distributions (PS50124 and PS606, respec-

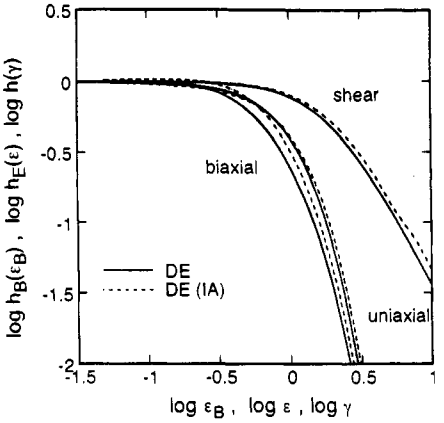

Figure 5. Summary of the Doi–Edwards predictions on damping functions in biaxial and uniaxial extensions and in shear.

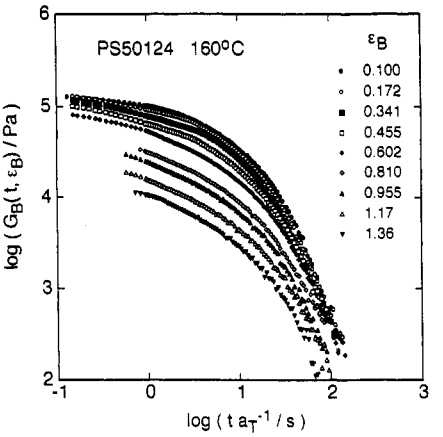

Figure 6. Biaxial relaxation modulus of narrow distribution PS50124 measured at various strains.

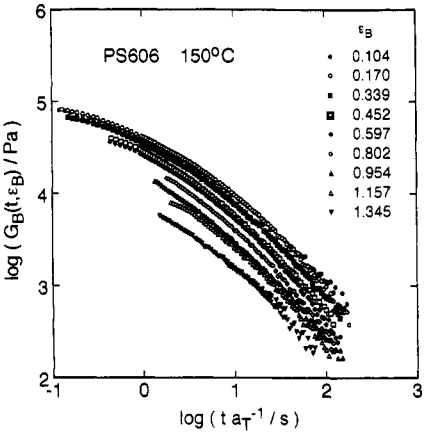

Figure 7. Biaxial relaxation modulus of broad distribution PS606 measured at various strains.

tively) were used for biaxial stress relaxation measurements. After the measurements, the weight-average molecular weights of PS50124 and PS606 are $M_w = 2.5 \times 10^5$ and 1.8×10^5, and polydisperse indices are $M_w/M_n = 1.1$ and 2.5, respectively. A somewhat broader molecular weight distribution was reported for PS50124 in the previous study.[8] Measurements of MWD by the GPC method for many samples after experiments of stress relaxations and extensional flows give an average value of $M_w/M_n = 1.1$ for PS50124.

III.2. Procedure in Biaxial Stress Relaxation. Equibiaxial stress relaxation measurements were made by applying the lubricated squeezing flow method with a biaxial extensional rheometer (BE-100, Iwamoto Seisakusho Co. Ltd.). The principle and operation of this new rheometer are similar to those reported previously.[8,16] Differences between the new and the previous rheometers are in the applicability of a step strain and the measurable range of thrust force up to 20 kg with the new rheometer. The maximum force was 10 kg in the previous rheometer. A step biaxial strain can be imposed by compressing the disk-shaped sample. The diameter of the parallel plates is 70 mm. The upper plate descends with a constant speed of 30 mm s^{-1}. The maximum change in sample thickness corresponding to the maximum strain is 5.6 mm. Thus, the time needed for imposition of a step strain (rise time) is less than 0.19 s. All stress relaxation data obtained within *ca.* 1 s at various temperatures are discarded, because the short time data are affected by the finite rise time. A potentiometer monitors the displacement of the upper plate, and a differential transformer and a pair of disk springs measure the thrust force. A microcomputer (NEC PC-9800) is used for data sampling, and its sampling rate is 0.01 s^{-1}.

The biaxial extensional strain ϵ_B is given by

$$\epsilon_B = -{}^1/_2 \ln(h/h_0) \tag{10}$$

assuming a uniform and ideal deformation for an incompressible material, where h_0 and h are the initial and final sample thicknesses, respectively. Neglecting the inertia force and surface tension, the net stress σ_B is evaluated from the thrust F by

$$\sigma_B \equiv |\sigma_{rr} - \sigma_{zz}| = F/A \qquad A = V/h \tag{11}$$

where V is the volume of a sample. The biaxial relaxation modulus is defined as

$$G_B(t,\epsilon_B) = \frac{\sigma_B}{\lambda_B^2 - \lambda_B^{-4}} = \frac{\sigma_B}{\exp(2\epsilon_B) - \exp(-4\epsilon_B)} \tag{12}$$

We prepared disk-shaped samples of 5–30 mm diameter and 5–6 mm height in a hot press holding at 170 °C for about 10 min. The sample size was determined according to the limitation of the measurable force. For measurement at a large strain the diameter should be small because of the upper limit of the measurable force, and for a small strain we used a large disk sample to increase the accuracy of the force measurement. The range of stretch ratio λ_B and strain ϵ_B for the biaxial measurements was 1.11–3.90 and 0.10–1.36. As a lubricant, we used silicone oil with the kinematic viscosity of 10 000 cSt (SH200, Toray Dow Corning Silicone, Inc.).

IV. Results and Discussion

IV.1. Biaxial Stress Relaxation. We measured the stress relaxation behavior of PS50124 and PS606 in equibiaxial extension and determined the biaxial relaxation modulus $G_B(t,\epsilon_B)$ from eq 12. The results are shown in Figures 6 and 7, respectively. From careful measurements, it was found that reproducibility of the modulus data is very good. The experimental scattering is within ±5% around average values except for data at long time ends. The time-temperature superposition principle can be applied to the modulus data which are obtained at the same strain and at different temperatures. Before the superposition, we discarded the short time data within *ca.* 1 s. Linear viscoelastic behavior is observed at $\epsilon_B < 0.17$ for both samples. The modulus data taken at $\epsilon_B = 0.10$ coincide with linear relaxation modulus data $G(t)$ obtained in the shear stress relaxation experiment. We cannot determine the equilibration time τ_{eq} from Figure 6 because the short time data are limited. In the previous study,[8] τ_{eq} was determined for PS50124 on the basis of the DE theory using shear stress relaxation data. The time τ_{eq} is 1.16 s, and at $t > 4.4\tau_{eq} = 5.1$ s the time–strain separability of the shear relaxation modulus $G(t,\gamma)$ is observed.[8] As we can see in Figure 6, the time–strain separability is also ap-

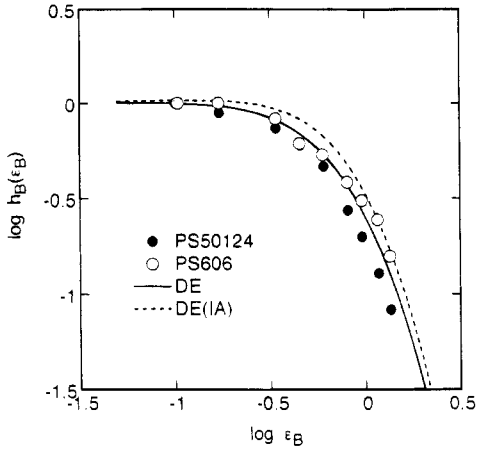

Figure 8. Comparison of the DE prediction with experimental data for biaxial damping function $h_B(\epsilon_B)$.

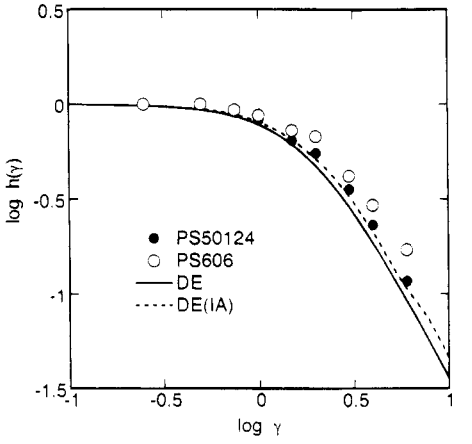

Figure 9. Comparison of the DE prediction with experimental data for shear damping function $h(\gamma)$.

plicable to the biaxial relaxation modulus $G_B(t,\epsilon_B)$ at $t \geq 5$ s for PS50124.

In Figure 8, the strain dependence of the damping function h_B is shown for the narrow- and broad-MWD samples. Stronger strain dependence is observed in the narrow distribution sample PS50124. The prediction of the DE theory (rigorous) for h_B agrees fairly well with the data for PS50124. However, the prediction obtained using the IA approximation is apparently higher than the data.

IV.2. Shear Stress Relaxation. Figure 9 shows shear damping functions $h(\gamma)$ for PS50124 and PS606. The damping function for PS50124 is obtained from the relaxation modulus data,[8] and the function for PS606 is obtained in the present study. Again the stronger strain dependence is observed for narrow PS. However, the difference in the strain dependence between narrow- and broad-MWD PS is smaller in shear than in biaxial extension. The DE predictions (both rigorous and IA) are close to the data for narrow-MWD PS.

IV.3. Uniaxial Extension. In general, it is hard to measure the nonlinear uniaxial stress relaxation behavior because of the difficulty in stretching the sample uniformly by a large step strain. For this reason, we tried to determine the uniaxial damping function $h_E(\epsilon)$ by following Wagner's method,[11,12] using data of stress growth coefficient $\eta_E^+(t,\dot{\epsilon})$ in uniaxial extension. Here, the coefficient $\eta_E^+(t,\dot{\epsilon})$ is defined by $\eta_E^+(t,\dot{\epsilon}) = \sigma_E(t)/\dot{\epsilon}$ with the net stretching stress $\sigma_E(t)$ and the strain rate $\dot{\epsilon}$. Wagner[11,12] derived the following equation from a

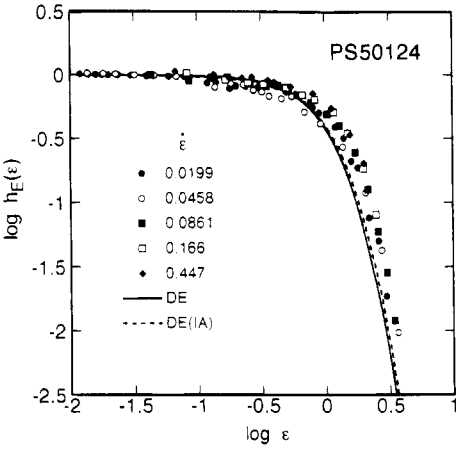

Figure 10. Comparison of the DE prediction with experimental data on narrow distribution PS50124 for uniaxial damping function $h_E(\epsilon)$.

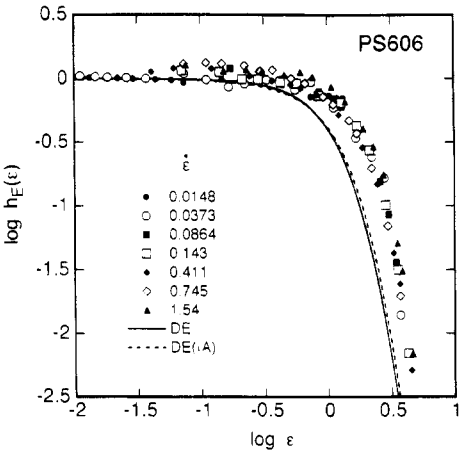

Figure 11. Uniaxial damping function $h_E(\epsilon)$ for broad distribution PS606.

general form of the BKZ constitutive equation,[13]

$$h_E(\dot{\epsilon}t) = \frac{\dfrac{\sigma_E(t)}{G(t)} - \displaystyle\int_0^t \sigma_E(s)\frac{m(s)}{G(s)^2}\,ds}{\exp(2\dot{\epsilon}t) - \exp(-\dot{\epsilon}t)} \qquad m(s) = -\frac{dG(s)}{ds} \tag{13}$$

Only the time–strain separability is assumed in the derivation. In eq 13, $m(s)$ is a memory function, which is a time derivative of the linear relaxation modulus $G(s)$ ($0 \leq s \leq t$). The product $\dot{\epsilon}t$ is the Hencky strain ϵ, and $h_E(\dot{\epsilon}t)$ ($=h_E(\epsilon)$) should be independent of $\dot{\epsilon}$. In this calculation we used $\eta_E^+(t,\dot{\epsilon})$ data measured under the condition of constant strain rate.

Figures 10 and 11 show damping functions $h_E(\epsilon)$ for PS50124 and PS606, respectively, which are calculated from $\eta_E^+(t,\dot{\epsilon})$ data.[8] In narrow-MWD PS50124, $h_E(\epsilon)$ is independent of $\dot{\epsilon}$ at $\dot{\epsilon} \leq (1.9\tau_{eq})^{-1} = 0.45\ s^{-1}$ within experimental scattering. This means that the independence of $h_E(\epsilon)$ on $\dot{\epsilon}$ is verified in the region where the time–strain separability holds, *i.e.*, at $\dot{\epsilon} \leq (4.4\tau_{eq})^{-1}$. The DE theory with and without the IA approximation gives almost the same prediction in uniaxial extension. This prediction agrees fairly well with the experimental data for PS50124.

On the other hand, for PS606 shown in Figure 11, all the data are almost on a composite curve. This is related to an ambiguity of the short time contraction

mode due to the broadness of the MWD in PS606. A comparison between Figures 10 and 11 clearly shows that the strain dependence of $h_E(\epsilon)$ becomes weaker in broad PS. The difference in strain dependence of damping functions between narrow and broad PS is the largest in uniaxial extension.

V. Conclusions

We have determined damping functions in shear, and uniaxial and biaxial extensions, for narrow- and broad-MWD PS samples in melts. The predictions of the DE theory agree fairly well with the data for the narrow distribution sample. For the broad distribution sample, weaker strain dependences of damping functions are observed for all the deformation modes.

References and Notes

(1) Osaki, K. *Rheol. Acta* **1993**, *32*, 429.
(2) Ferry, J. D. *Viscoelastic properties of polymers*, 3rd ed.; Wiley: New York, 1980.
(3) Doi, M.; Edwards, S. F. *J. Chem. Soc., Faraday Trans. 2* **1978**, *74*, 1802.
(4) Doi, M. *J. Polym. Sci.* **1980**, *18*, 1005.
(5) Doi, M.; Edwards, S. F. *The Theory of Polymer Dynamics*; Oxford University Press: Oxford, U.K., 1986.
(6) Larson, R. G. *J. Rheol.* **1984**, *28*, 545.
(7) Marrucci, G. *J. Rheol.* **1983**, *27*, 433.
(8) Takahashi, M.; Isaki, T.; Takigawa, T.; Masuda, T. *J. Rheol.* **1993**, *37*, 827.
(9) Soskey, P. R.; Winter, H. H. *J. Rheol.* **1985**, *29*, 493.
(10) Khan, S. A.; Prud'homme, R. K.; Larson, R. G. *Rheol. Acta* **1987**, *26*, 144.
(11) Wagner, M. H. *Rheol. Acta* **1990**, *29*, 594.
(12) Wagner, M. H.; Demarmels, A. *J. Rheol.* **1990**, *34*, 943.
(13) Larson, R. G. *Constitutive Equations for Polymer Melts and Solutions*; Butterworths: Boston, 1988.
(14) Demarmels, A.; Meissner, J. *Colloid Polym. Sci.* **1986**, *264*, 829.
(15) Sekiyo, M.; Doi, M. *J. Phys. Soc. Jpn.* **1982**, *51*, 3672.
(16) Golshan Ebrahimi, N.; Takahashi, M.; Araki, O.; Masuda, T. *Acta Polym.* **1995**, *46*, 267.

MA950307W